

The carbonate content in high-temperature apatite: An analytical method applied to apatite from the Jacupiranga alkaline complex

ROBERTO V. SANTOS*

Department of the Geophysical Sciences, University of Chicago, 5734 South Ellis Avenue, Chicago, Illinois 60637, U.S.A.

ROBERT N. CLAYTON

Department of the Geophysical Sciences, Department of Chemistry, and Enrico Fermi Institute, University of Chicago, 5640 South Ellis Avenue, Chicago, Illinois 60637, U.S.A.

ABSTRACT

We present a method to measure carbonate content of apatite that uses infrared spectroscopy. The method was calibrated against the amount of CO₂ released by reaction of apatite with phosphoric acid and may be used to study apatite with CO₂ content below 1 wt%. We have applied the method to apatite from carbonatite (≈ 0.3 – 0.4 wt% CO₂) and metasomatic (≈ 0.6 – 1.0 wt% CO₂) and alkaline silicate (< 0.3 wt% CO₂) rocks from the Jacupiranga alkaline complex. The results show that higher concentration of carbonate was found in apatite related to metasomatic processes and, in particular, to metasomatism related to the intrusion of carbonatite from Jacupiranga. Major and trace elements of the analyzed apatites do not show a simple substitution mechanism that would explain the presence of carbonate in the apatite structure.

In a series of exploratory laboratory experiments in which apatite was synthesized under high temperature and pressure, no clear relationship was observed between the carbonate content of the synthetic apatite and the total C content in the coexisting fluid (molecular CO₂ or carbonate ions in solution). However, even though these experiments were not conclusive, they suggest that apatite coexisting with carbonate ions in solution has a CO₂ content above 0.3 wt%, whereas apatite coexisting with molecular CO₂ has a CO₂ content < 0.3 wt%. These results indicate that the CO₂ content of apatite depends not only on total fluid C content, but also on the C speciation in the fluid.

INTRODUCTION

Apatite is a common accessory mineral in sedimentary, metamorphic, and igneous rocks and may be described as a solid-solution series in which the end-members are hydroxylapatite, chlorapatite, fluorapatite, and carbonate-apatite. Besides the carbonate-apatite, which may have up to 7 wt% CO₂, OH-, F-, and Cl-bearing apatites are also known to have trace amounts of carbonate, as indicated by the carbonate content in high-temperature apatites, which usually have < 1.0 wt% CO₂ (LeGeros, 1965; Prins, 1973; Sommerauer and Katz-Lehnert, 1985; Binder and Troll, 1989).

Methods to measure the CO₃²⁻ in apatites include thermogravimetric methods (Holager, 1972), differential thermal analysis (Silverman et al., 1952), gas-solid chromatography (Nelson and Featherstone, 1982), and reaction with phosphoric acid (Groves, 1951). These methods require either a large amount of sample or a specifically constructed apparatus, which in many cases must also be properly calibrated. The use of infrared (IR) spectroscopy to measure CO₃²⁻ in apatites was reported by Arends and

Davidson (1975), who showed a good relationship between the transmittance of the carbonate band and the amount of carbonate analyzed chemically. However, the absence of internal standardization and difficulties in sample preparation led to analytical problems (e.g., inaccurate sample and KBr weights and heterogeneity of the pellets). An internal standardization method using IR spectrometry was introduced by Featherstone et al. (1984), who normalized the extinction of the carbonate band at about 1415 cm⁻¹, using the phosphate band at about 575 cm⁻¹, and argued that such a normalization is linearly related to the carbonate content in the apatite structure for carbonate contents in the range of 1–12 wt%. They also mentioned that with decreasing carbonate content this relation becomes less reliable.

We have studied the carbonate content in apatite structure from carbonatites and alkaline silicate rocks using Fourier-transform infrared spectroscopy (FTIR). We developed an internally normalized method to measure the carbonate content of apatite, which is similar to that described by Featherstone et al. (1984). The method was calibrated against the amount of CO₂ released by reacting apatite with 100% H₃PO₄ and may be useful in studying the carbonate content in high-temperature apatite. We have applied the method to apatite from alkaline silicate

* Present address: Dep. de Geologia, Universidade Federal de Ouro Preto, 35400, Ouro Preto-MG, Brazil.

TABLE 1. Vibration frequencies (cm^{-1}) of hydroxylapatite and fluorapatites

Compound	Ref.	ν_1	ν_2	ν_3	ν_4	$\nu(\text{OH})$	Libration (OH)
$\text{Ca}_5(\text{PO}_4)_3\text{F}$	*	960	315, 270	1095, 1075, 1040	603, 574, 566		
$\text{Ca}_5(\text{PO}_4)_3\text{F}$	**	968	325	1096, 1050, 1025	605, 580, 565		
$\text{Ca}_5(\text{PO}_4)_3\text{OH}$	*	962	350, 270	1092, 1065, 1028	603, 574, 564	3566	633
$\text{Ca}_5(\text{PO}_4)_3\text{OH}$	†	962	255	1095, 1055, 1035	605, 568	3578	635

* Baddiel and Berry (1966).
 ** Bhatnagar (1967).
 † Bhatnagar (1968).

rocks and carbonatites and show that they usually have <1.0 wt% CO_2 . We also present a summary of laboratory experiments in which apatite has been synthesized under different pressure and temperature conditions and in the presence of fluids with different chemical composition and CO_2 - H_2O ratios.

THE INFRARED SPECTRUM OF APATITE

The IR spectrum of apatite is characterized by three main regions, which are related to the vibration frequencies of the OH^- , CO_3^{2-} , and PO_4^{3-} ions. Table 1 shows the vibration frequency of PO_4^{3-} and OH^- ions for fluorapatite and hydroxylapatite. The phosphate ion has the following vibration frequencies: a symmetric stretch (ν_1), a double degenerate symmetric bend (ν_2), a triply degenerate asymmetric stretch (ν_3), and a triply degenerate asymmetric bend (ν_4) (Fig. 1). The asymmetric vibrations are both infrared and Raman active, whereas the symmetric ones are mostly Raman active. In hydroxylapatites the OH^- vibration bands occur at 3572 and 634 cm^{-1} , whereas in F-bearing apatites the band at 3572 cm^{-1} is shifted to 3534 cm^{-1} and the band at 634 cm^{-1} is shifted to 747 cm^{-1} (Freund and Knobel, 1977). Okazaki (1983) noted that the degree of fluoridation also affects the CO_3^{2-} vibration frequency at 875 cm^{-1} , shifting it to lower frequencies.

The infrared spectrum of apatite depends on the substitution mechanism of CO_3^{2-} in the apatite structure. According to Elliott (1965) and Bonel and Montel (1964), apatite in which the carbonate replaces the PO_4^{3-} (apatite type B) has infrared CO_3^{2-} bands at 864, 1430, and 1455 cm^{-1} (Fig. 1), whereas apatite in which the carbonate replaces the OH^- (apatite type A) has CO_3^{2-} bands at 883, 1465, and 1542 cm^{-1} . Elliott (1965) also showed that, compared with the free carbonate ion, the carbonate ion in apatite is distorted and that although the carbonate ion of apatite type B is oriented parallel to the *c* axis, the carbonate ion of apatite A is approximately perpendicular to the *c* axis. The apatites being studied here and most apatites are type B. Their carbonate infrared band may be distinguished from that of carbonate minerals by its double peak in the 1440- cm^{-1} region. The free carbonate ion has six modes of vibration (White, 1974): a symmetric stretching vibration (ν_1), an out of plane vibration (ν_2), a doubly degenerate asymmetric stretch (ν_3), and a doubly degenerate bending mode (ν_4). Among those vibration modes, the strongest infrared peak in calcite is

the asymmetric stretch ν_3 near 1440 cm^{-1} . Besides the band at 1440 cm^{-1} , calcite also has infrared bands at 1800, 872, and 710 cm^{-1} .

MEASUREMENT OF CARBONATE CONTENT IN APATITE USING FTIR

Samples

The samples used in the calibration procedure are all apatites that were separated by conventional heavy liquid and magnetic methods (in a Frantz isodynamic magnetic separator). The Egan and Front samples, which are large apatite crystals (>2 cm), belong to the University of Chicago mineral collection and are, respectively, from Eganville and Frontenac, Ontario, Canada. Samples C4-3B, C4-3E, and C1-2A are from carbonatite, and sample 235-2CCE is from an olivine monzonite, all from the Jacupiranga alkaline complex, Brazil. Samples TP-90-13A and BTP-90-13A are from the Tapira alkaline complex, Brazil, and were separated from a rock in which the main minerals are apatite, phlogopite, and magnetite. Besides the samples above, this study also presents the CO_2 content of apatite from rocks of the Jacupiranga alkaline complex, which were separated using the same procedure as above.

The apatites were analyzed for major and trace elements with a Cameca SX-50 microprobe set to a 25-nA sample current and a 15-kV accelerating voltage (Table

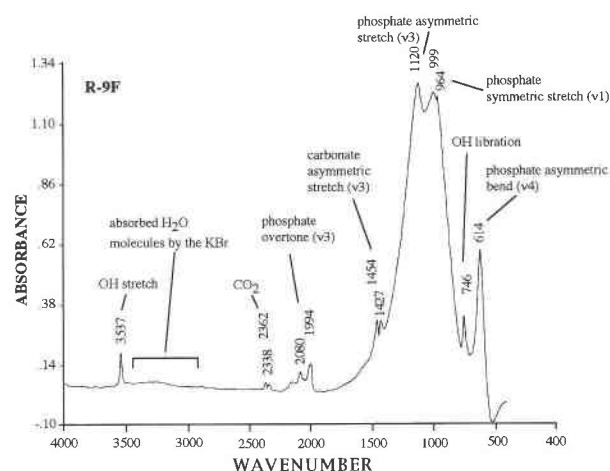


Fig. 1. Infrared spectrum of apatite (R-9F) between 400 and 4000 cm^{-1} . CO_2 concentration of 0.13 wt%.

TABLE 2. Chemical composition of apatites

	17FEB93-B*	TP90**	M4REAC4**	M4V†	C4-3B†	R-9A‡	R-2B‡	R-2K‡	235-2CCE‡	R-16B‡
SiO ₂	0.10	0.21	0.01	0.22	0.02	0.27	0.60	0.42	0.25	0.84
FeO	0.02	0.03	0.07	0.24	0.03	0.09	0.03	0.13	0.20	0.27
MnO	0.01	0.00	0.02	0.02	0.01	0.01	0.01	0.01	0.06	0.01
MgO	0.01	0.01	0.05	0.01	0.13	0.03	0.01	0.01	0.06	0.01
CaO	35.42	55.09	54.58	54.65	54.97	54.15	54.32	54.63	54.37	53.67
SrO	0.29	0.93	0.51	0.35	0.40	1.12	1.27	0.87	0.16	0.29
Ce ₂ O ₃	0.00	0.11	0.12	0.50	0.04	0.33	0.30	0.33	0.59	1.29
Na ₂ O	19.29	0.01	0.07	0.13	0.13	0.03	0.09	0.00	0.08	0.11
K ₂ O	0.00	0.00	0.01	0.02	0.00	0.00	0.01	0.01	0.00	0.04
P ₂ O ₅	46.39	42.08	42.50	42.37	42.94	42.84	40.84	42.79	42.22	40.66
SO ₃	0.01	0.02	0.01	0.03	0.03	0.00	0.01	0.08	0.00	0.08
F	0.02	1.48	1.39	1.54	1.20	2.13	1.84	2.02	2.29	2.71
Cl	0.00	0.00	0.00	0.01	0.01	0.38	0.15	0.01	0.54	0.01
Total	101.56	99.99	99.33	100.08	99.91	101.40	99.47	101.31	100.84	99.99

* Synthetic.

** Magnetite + phlogopite + apatite-bearing rock.

† Carbonatites.

‡ Silicate rocks.

2). In order to avoid excess volatile loss, the electron beam was defocused to a beam size of 15 μm . The detection level of the elements is 100 ppm, except for Sr and Ce, which have a detection level of 300 ppm. According to Stormer et al. (1993), microprobe measurements of apatite should be interpreted with caution because of F and Cl diffusion during analysis, which depend, among other factors, on the crystallographic orientation of the analyzed grain. They reported that the largest variations in $FK\alpha$ and $ClK\alpha$ X-ray radiation were observed on surfaces perpendicular to the *c* axis and produced increases in X-ray intensity up to 100% during the first 60 s of exposure to the beam. These microprobe data should be regarded as approximate compositions; however, they are important in the evaluation of the need of correction in the peak area of the FTIR spectrum because of variations in chemical composition of the apatites.

Apatite is an accessory mineral that can be easily separated from most common minerals. It has specific gravity of 3.1 g/cm³, greater than that of minerals such as quartz and feldspars, and it has a very low magnetic susceptibility, which makes it easy to separate from micas, carbonates, and magnesium iron silicates. In the present study, 1–2 g of apatite was concentrated from each sample. Such a large amount of sample was necessary because of the calibration method used. Once concentrated, the samples were observed under the microscope to detect possible carbonate contamination. Contamination by carbonate minerals is a potential problem in the method presented here because of the coexistence of apatite and carbonates in many instances. Carbonate contamination may be recognized by the shape of the CO₃²⁻ absorption peak in the 1440 cm⁻¹ region, as well as by observing grain-mounted thin sections under the microscope. The samples studied here were observed under the microscope and showed no evidence of carbonate contamination. Unlike apatite, carbonates typically have a single peak in the 1440-cm⁻¹ region of the infrared spectra, and they also have a much higher optical birefringence.

Measurement of the CO₂ released by reaction with H₃PO₄

The reaction of apatite with phosphoric acid followed a procedure similar to the extraction of CO₂ from carbonates for isotopic analysis (McCrea, 1950). Seventy to 150 mg of sample was placed in phosphoric acid using double-vessel reaction tubes, which, once loaded, were outgassed on a vacuum line. The reaction tubes were placed in a bath at 50 °C for 15 min before the acid was introduced to the sample. Each apatite had a different reaction rate and, in particular, the carbonate-rich apatites typically reacted faster than the carbonate-poor ones. In some cases, such as sample 235-2CCE, the reaction was very slow, and a significant amount of residue was observed even after 24 h of reaction. In such cases, the reaction tubes were heated until all the sample reacted completely. The CO₂ was extracted in a vacuum line and its volume measured in a Hg column. Because no residue was observed in the reaction vessels, it was assumed that the yields of CO₂ were nearly 100%.

Infrared measurements

The IR spectra were obtained using a Nicolet 60SX FTIR spectrometer adapted with microsample chamber and a continuous dry N₂ gas purge. The sample preparation followed the general procedure described in the literature (Fridmann, 1967; Nelson and Featherstone, 1982). Approximately 5 mg of finely ground sample (ground under acetone in an agate mortar) and 360 mg of KBr were mixed and placed in a desiccator overnight at 110 °C. The pellets (KBr + apatite) were prepared in a die with a 1.27-cm diameter under vacuum with a total pressure of 8 ton per square inch (8 kbar). The die was held at maximum pressure for 3–4 min, after which the vacuum pump was turned off and the pressure released. After compression, the pellets were immediately stored in a desiccator (at room temperature) to avoid absorption of atmospheric H₂O.

The samples were scanned using a KBr beam splitter

TABLE 3. Samples, average values, and standard deviation (in parentheses) used in the calibration procedure

Sample	H*	C*	P*	H/P	C/P	wt% CO ₂ **
235-2CCE	1.39 (0.06)	1.28 (0.02)	382.50 (74.39)	3.69×10^{-3} (5.59×10^{-3})	3.42×10^{-3} (6.08×10^{-3})	0.06
C4-3B	5.66 (0.39)	7.66 (0.23)	248.23 (5.67)	2.28×10^{-2} (1.18×10^{-3})	3.09×10^{-2} (2.52×10^{-4})	0.31
C1-2A	5.47 (0.15)	10.07 (0.23)	260.53 (1.99)	2.10×10^{-2} (4.00×10^{-4})	3.86×10^{-2} (6.03×10^{-4})	0.40
C4-3E	6.95 (0.22)	13.41 (0.34)	305.23 (2.86)	2.28×10^{-2} (5.13×10^{-4})	4.39×10^{-2} (1.04×10^{-3})	0.41
FRONT	0.95 (0.02)	18.09 (0.21)	326.4 (4.98)	2.90×10^{-3} (2.08×10^{-5})	5.54×10^{-2} (3.21×10^{-4})	0.46
EGAN	1.41 (0.06)	18.71 (0.25)	335.45 (1.20)	4.19×10^{-3} (1.84×10^{-4})	5.58×10^{-2} (9.19×10^{-4})	0.51
TP-90-13	7.11 (0.17)	25.03 (0.43)	310.78 (14.28)	2.29×10^{-2} (1.51×10^{-3})	8.07×10^{-2} (3.94×10^{-3})	0.67
BTP-90-13	8.07 (0.06)	25.22 (0.28)	313.7 (1.41)	2.57×10^{-2} (7.07×10^{-5})	8.04×10^{-2} (5.66×10^{-4})	0.67

* Areas under the OH (H \approx 3530–3570 cm⁻¹), CO₃²⁻ (C \approx 1430–1470 cm⁻¹), and PO₄³⁻ (P \approx 700–1420 cm⁻¹) peaks, measured using software with base-line correction.

** CO₂ concentration in apatites measured by reaction of the samples with phosphoric acid.

and MCTA detector, which gives a configuration effective for radiation between 4000 and 400 cm⁻¹ and includes the main phosphate band at 1050 cm⁻¹. They were scanned at least twice and were normalized against a pure KBr pellet. Once the samples were scanned, the areas under the OH⁻ (H \approx 3530–3570 cm⁻¹), CO₃²⁻ (C \approx 1430–1470 cm⁻¹), and PO₄³⁻ (P \approx 700–1420 cm⁻¹) peaks were measured using base-line correction. The values of these areas, denominated H, C, and P, are presented in Table 3. The wavelength interval under the carbonate and phosphate peaks varies from sample to sample and may depend, among other factors, on the chemical composition of the sample and its carbonate content. These intervals were determined visually and the base lines were placed approximately between 1430 and 1470 cm⁻¹ (the area under the carbonate peak) and 700 and 1420 cm⁻¹ (the area under the phosphate peak). Table 3 also shows the ratios H/P and C/P, which are used in the internal normalization method applied to the data. The ratio C/P varies from sample to sample and ranges between 0.003 and 0.08. The basis of the method presented here is that this ratio is proportional to the concentration of carbonate within the apatite structure. It should be noted that in the P region there are also a carbonate peak (\approx 870 cm⁻¹) and SiO₂ vibration frequencies, which are assumed to have a negligible area compared with the total P area.

The C/P ratio was calibrated using the amount of CO₂ released in the reaction between apatite and phosphoric acid, as described above. The average C/P and the carbonate content of each sample are presented in Table 3 and in Figure 2, which shows that the data fit well to a second-order polynomial ($y = 0.032334 + 9.6301x - 21.915x^2$; $R^2 = 0.991$) that does not pass through the origin. Although the data also fit a straight line reasonably well ($y = 0.0638 + 7.6573x$; $R^2 = 0.985$), the intercept of the second-order polynomial is closer to the origin. At this point, it is not clear why the second-order polynomial regression fits the data better.

INFRARED SPECTRA OF APATITE AND ITS CARBONATE CONTENT

The apatite samples from the silicate rocks from Jacupiranga were analyzed for CO₂ according to the spectroscopic procedure described above. The infrared spectra are similar to those shown previously and are characterized by a OH⁻ band at 3530 cm⁻¹, CO₃²⁻ bands at 1460, 1430, and 880 cm⁻¹, and PO₄³⁻ bands at 1093, 1075, and 1040 cm⁻¹. The infrared band at 880 cm⁻¹ was observed only in those samples with CO₂ contents higher than 0.2 wt%, such as samples C1-2A and Reac-6. Table 4 and Figure 3 show the rock types from which the samples were obtained, as well as the measured concentration of CO₂ within the apatites. The CO₂ content of these apatites, which ranges from 0.06 to 0.8 wt%, seems to depend on the apatites' geological environment. For instance, apatites from alkaline silicate rocks that do

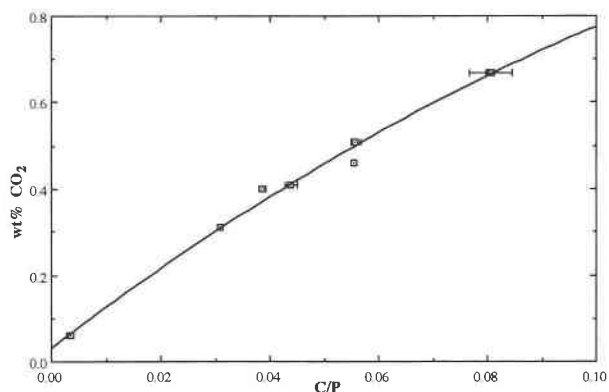


Fig. 2. Plot of the ratio C/P vs. the content of CO₂ within the apatite measured by reaction with phosphoric acid. The values of ratio C and P represent, respectively, the areas of the carbonate (C = 1470–1430 cm⁻¹) and phosphate (P = 700–1420 cm⁻¹) peak of the infrared spectrum of apatite. This figure also shows the error bar of the ratio C/P for each sample.

TABLE 4. CO₂ contents of apatite from carbonatite and silicate rocks measured by FTIR

Sample	Rock	wt% CO ₂
C1-2A*	Carbonatite	0.37
C4-3B*	Carbonatite	0.41
J-1C	Ijolite	0.27
R-9A	Magnetite clinopyroxenite	0.17
R-9F	Magnetite clinopyroxenite with phlogopite	0.13
J-223-04	Melteigite	0.10
R-2B	Melteigite	0.80
R-2K	Melteigite	0.33
235-2CCE	Olivine gabbro	0.06
BTP-90-13A*	Reaction zone rock	0.67
REAC-6*	Reaction zone rock	0.68
R-16B	Syenite	0.07

* Samples in which apatite coexists with carbonate minerals, mainly calcite.

not show signs of carbonate or alkaline metasomatism have CO₂ contents below 0.3 wt% (Fig. 4), whereas apatites from carbonatites or related to alkaline silicate rocks partially affected by fenitizing solutions show CO₂ contents ranging between 0.3 and 0.5 wt% (Fig. 5). A third group of apatites, which have CO₂ contents above 0.5%, occurs in a metasomatic coarse-grained rock in which the main minerals are magnetite, phlogopite, calcite, and apatite (Fig. 6) and in a melteigite that has been affected by feldspathic fenitization.

LABORATORY EXPERIMENTS AT HIGH TEMPERATURE AND PRESSURE

This section describes the results of laboratory experiments in which apatite was synthesized under different pressure and temperature conditions. In order to evaluate the effects of CO₂ speciation of the fluid on the CO₂ content of apatite, these experiments were performed using both molecular CO₂-bearing fluids and carbonate ions in solution. It should be emphasized that, because these experiments are exploratory, they give only general guide-

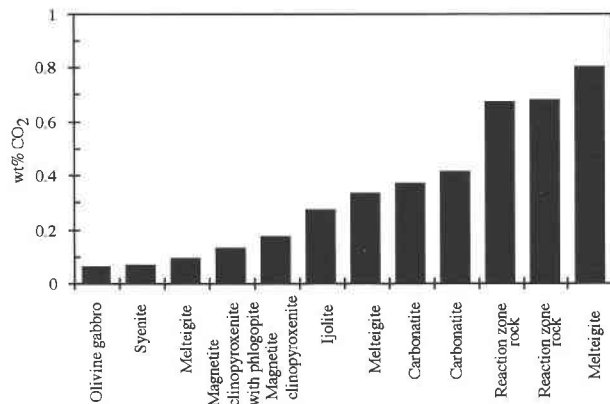


Fig. 3. CO₂ content of apatites from the silicate rocks from Jacupiranga measured by infrared spectrometry. The higher CO₂ concentrations were observed in apatites related to metasomatic processes.

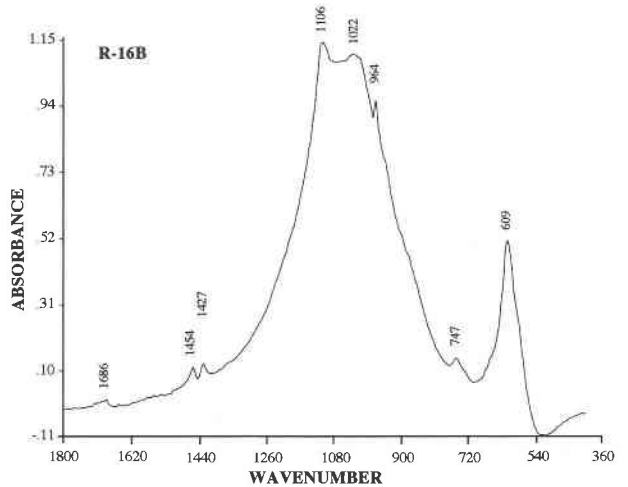


Fig. 4. Infrared spectrum of apatite from syenite. CO₂ concentration of 0.07 wt%.

lines for future studies and were not performed under controlled conditions of f_{O_2} and f_{H_2} . Table 5 summarizes the experiments in terms of composition, pressure, and temperature conditions of the charges. With the exceptions of Reactions 1 and 2, which were performed in a Morey pressure vessel, all experiments were made using Au or Pt capsules loaded into either cold-seal vessels (pressure below 3 kbar) or a piston-cylinder apparatus (pressure of 12 kbar). The starting materials were not checked by XRD, and the experiment products were studied using XRD, FTIR and, in some instances, SEM.

The hydroxylapatite grains produced in Reactions 1, 2, and 3 have CO₂ contents between 0.11 and 0.35 wt%. The presence of CO₂ in the apatite of the experiment product of Reaction 2 has been interpreted as due to carbonate contamination during the experiment. The experiment products had well-defined apatite X-ray peaks and consisted of acicular grains of apatite, which usually formed aggregates of 50–100 μm . The experiment products of Reactions 1 and 2 were used as starting materials in experiments involving hydroxylapatite and H₂O-CO₂ fluids at 2 kbar and 500 °C (Reactions 4–7 of Table 5), which showed that independent of the CO₂-H₂O ratio of the fluid, the resulting apatite had CO₂ contents below 0.2 wt%. For the experiments in which the starting material had 0.35 wt% CO₂ (Reactions 4 and 5), a decrease in the CO₂ content of the experiment product was observed relative to that of the starting material. Table 5 also presents the results of Reactions 8 and 9, in which apatite from Reaction 1 reacted with CaCO₃ and dehydrated oxalic acid, respectively, at pressures of 12 kbar and 900 °C. The experiment products of both reactions consisted of submillimeter-sized acicular apatite grains that may have been crystallized from a melt. The infrared spectra of these apatites showed no carbonate peaks.

A similar set of experiments was performed using fluorohydroxylapatite instead of hydroxylapatite. The fluo-

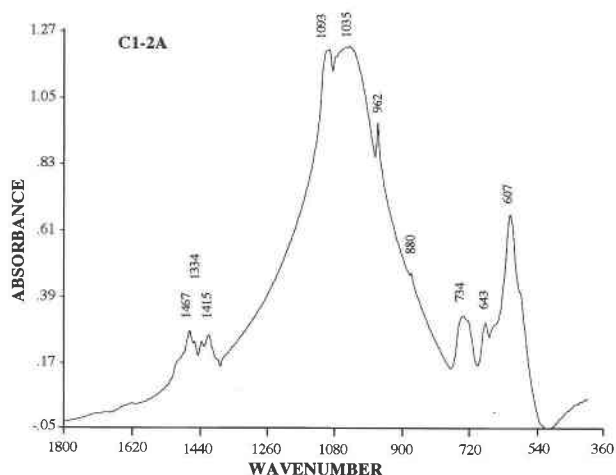


Fig. 5. Infrared spectrum of apatite from carbonatite. CO₂ concentration of 0.37 wt%.

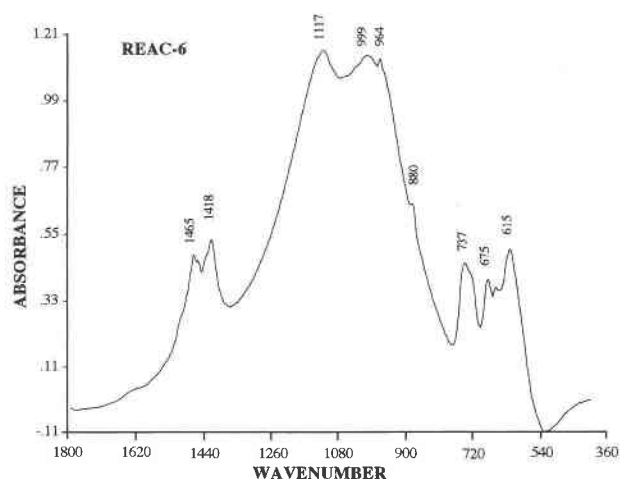


Fig. 6. Infrared spectrum of apatite from a reaction zone rock. CO₂ concentration of 0.68 wt%.

rohydroxylapatite was synthesized at 1 kbar and 800 °C by reacting Ca₃(PO₄)₂, CaF₂, and H₂O in the presence of H₂O (Reaction 10) and H₂O-CO₂ (Reaction 11), as well as at 2 kbar and 800 °C by reacting Ca₃(PO₄)₂, CaF₂, and Na₂CO₃ in the presence of H₂O and CO₂ (Reaction 12). Among these experiments, the only one that produced carbonate-bearing apatite was Reaction 12 (0.36 wt% CO₂), the infrared spectrum of which is shown in Figure 7. When the infrared spectrum of the hydroxylapatite from Reaction 1 (Fig. 8) is compared with that of Reaction 12, one observes the following differences: (1) the OH⁻ stretching peak at 3571 cm⁻¹ in the hydroxylapatite was shifted to 3538 cm⁻¹ in the fluorohydroxylapatite; (2) the OH⁻ libration peak at 636 cm⁻¹ in the hydroxylapatite was shifted to 745 cm⁻¹ in the fluorohydroxylapatite; (3) probably because of fluid inclusions, the infrared spectrum of the hydroxylapatite also shows a molecular CO₂ peak. Besides the carbonate peaks of apatite type B (1458

and 1414 cm⁻¹), apatite from Reaction 1 also has a peak at 1549 cm⁻¹, which may be related to the presence of apatite type B. Compared with the hydroxylapatite peaks, the OH⁻ peak in the fluorohydroxylapatite is much smaller, and it occurs at 3538 cm⁻¹, in agreement with previous observations of Freund and Knobel (1977).

In order to evaluate the effects of other cations within the apatite structure, hydroxylapatite was synthesized by reaction of Ca₃(PO₄)₂ with Na₂CO₃ at 400 °C and 2 kbar, under H₂O-CO₂ pressures (Reactions 13–17 of Table 5). The experiment products consisted of two generations of crystals: one generation of acicular apatite crystals similar to those of Reaction 1; and another generation of tabular crystals identified by X-ray diffractometry as β-NaCaPO₄ and previously reported in high-temperature experiments (Ando and Matsuno, 1968). Infrared analyses of the experiment product of Reactions 13–17 gave different results in terms of CO₂ concentration in the phosphates,

TABLE 5. Summary of the laboratory experiments

Reaction	Sample	Charge	T (°C)	P (kbar)	t (h)	wt% CO ₂ *	wt% CO ₂ **
1	27JAN92-I	CaCO ₃ + (NH ₄)H ₂ (PO ₄) + H ₂ O	350–450	n.d.	24		0.35
2	02FEB92-I	(NH ₄)H ₂ (PO ₄) + CaO + H ₂ O	350–450	n.d.	24		0.11
3	31JAN93-I	Ca ₃ (PO ₄) ₂ + CaCO ₃ + H ₂ O	400	2	168		0.36
4	12FEB92-1	ApaRun27JAN92-I + AnOac	518	2	24		0.14
5	12FEB92-2	ApaRun27JAN92-I + HyOac	514	2	120		0.13
6	12FEB92-3	ApaRun02FEB92-I + HyOac	518	2	24		0.10
7	12FEB92-4	ApaRun02FEB92-I + AnOac	518	2	24		0.22
8	15APR92-I	ApaRun27JAN92-I + CaCO ₃	900	12	21		n.c.
9	4MAY92-I	ApaRun27JAN92-I + AnOac	900	12	20		n.c.
10	17NOV92-I	Ca ₃ (PO ₄) ₂ + CaF ₂ + H ₂ O	810	1	24		n.c.
11	17NOV92-II	Ca ₃ (PO ₄) ₂ + CaF ₂ + HyOac	810	1	24		n.c.
12	30NOV92-I	Ca ₃ (PO ₄) ₂ + Na ₂ CO ₃ + CaF ₂ + HyOac	810	2	48		0.36
13	17FEB93-A	Ca ₃ (PO ₄) ₂ + Na ₂ CO ₃ + HyOac	400	2	264	0.62	0.40
14	10FEB93-II	Ca ₃ (PO ₄) ₂ + Na ₂ CO ₃ + HyOac	400	2	60	0.76	
15	17FEB93-B	Ca ₃ (PO ₄) ₂ + Na ₂ CO ₃ + HyOac	400	2	264	1.12	0.38
16	10FEB93-I	Ca ₃ (PO ₄) ₂ + Na ₂ CO ₃ + HyOac	400	2	60	2.22	
17	31JAN93-III	Ca ₃ (PO ₄) ₂ + Na ₂ CO ₃ + HyOac	400	2	144	2.71	

Note: n.d. = not determined; n.c. = no carbonate peak; AnOac = anhydrous oxalic acid; HyOac = hydrous oxalic acid.

* Experiment product washed with H₂O prior to analysis.

** Experiment product washed with acetic acid 2N prior to analysis.

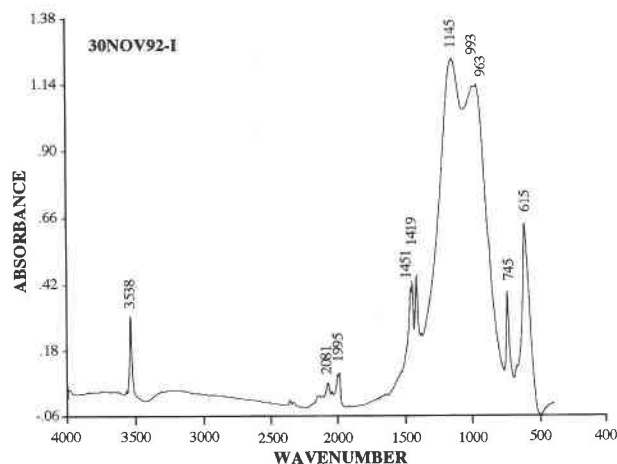


Fig. 7. Infrared spectrum of synthetic fluorohydroxylapatite. CO₂ content of 0.36 wt%.

depending on whether the samples were washed with 2*N* acetic acid or H₂O prior to the analysis. Samples treated with acetic acid revealed CO₂ concentrations of 0.36 wt%, whereas samples that were washed with water showed prominent double-carbonate peaks, similar to those in carbonate-bearing apatite, and gave CO₂ concentrations up to 2.8 wt%. It is possible that besides the presence of β-NaCaPO₄, other phosphate phases might have formed in these reactions, which would explain the high contents of CO₂ observed in the infrared analyses.

DISCUSSION

Most studies on high-temperature apatite indicate that they have <1 wt% CO₂ in the structure (Gulbrandsen et al., 1966; Prins, 1973; LeBas and Handley, 1979; Sommerauer and Katz-Lehnert, 1985; Binder and Troll, 1989). These studies applied methods such as thermogravimetric methods, differential thermal analysis, gas-solid chromatography, and reaction with phosphoric acid. Compared with the method presented here, these methods require either a large amount of sample or a specifically constructed apparatus. Binder and Troll (1989) reported analyses of apatite in which the minor elements (F, Cl, OH, and C) were obtained by wet-chemical methods and showed that the CO₂ contents of apatite from carbonatite samples range between 0.31 and 0.95 wt%, similar to the results of this study. Apatites of this study also have CO₂ contents and a chemical composition comparable with those reported by LeBas and Handley (1979), who studied apatite in carbonatites by microprobe. Because there is no simple relationship between the chemical composition of apatite and fluid composition, it is not clear whether the high values of F in apatites from the silicate rocks are related to a high-F activity in coexisting fluid or to the chemical composition of the fluid (e.g., the CO₂-H₂O ratio).

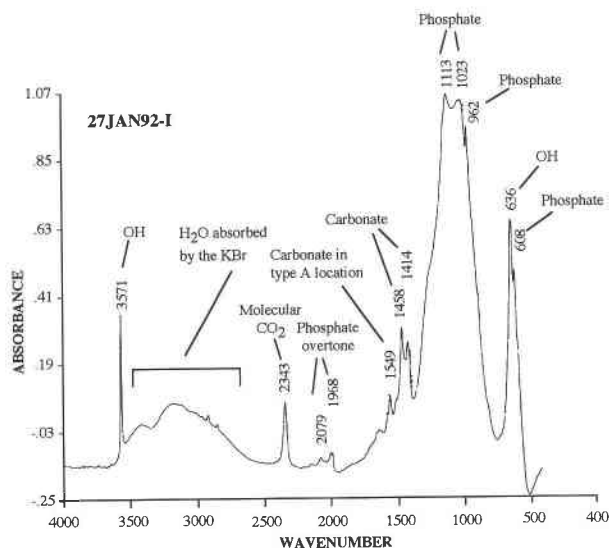


Fig. 8. Infrared spectrum of synthetic hydroxylapatite. CO₂ content of 0.35 wt%.

There have been discussions in the literature about the mechanisms of introducing CO₃²⁻ into the apatite structure. Commonly suggested mechanisms for substitution are the replacement of PO₄³⁻ ions by CO₃²⁻ plus a negative ion (i.e., F⁻ or OH⁻; Prins, 1973; Sommerauer and Katz-Lehnert, 1985; Binder and Troll, 1989) or by CO₃²⁻ with concomitant replacement of Ca²⁺ by a univalent positive ion (i.e., Na⁺; Ames, 1959; LeGeros et al., 1968; Nelson and Featherstone, 1982). Evidence pointing to the replacement of PO₄³⁻ by CO₃²⁻ includes a negative correlation between the carbonate content of apatites and their *a*-axis dimension (LeGeros, 1965; Binder and Troll, 1989) and a negative correlation between the carbonate and phosphate contents in apatite (McClellan and Lehr, 1969; Chickerur et al., 1980; Nelson and Featherstone, 1982; Binder and Troll, 1989). LeGeros et al. (1968) have also suggested that carbonate in apatite may be explained by replacement of 2(OH⁻) by CO₃²⁻, or PO₄³⁻ by (CO₃OH)³⁻, or Ca₅PO₄ by CO₃²⁻. Binder and Troll (1989) stated that Ca-O trigonal prism columns in apatite, which are positioned parallel to the *c* axis, are linked laterally to tetrahedral phosphate polyhedra by sharing one edge. They argued that in F-bearing apatite the partial replacement of the phosphate tetrahedra by a smaller tetrahedral CO₃F group would reduce the lateral distance between the Ca-O trigonal prism columns and, consequently, the *a*-axis dimension. Sommerauer and Katz-Lehnert (1985) presented a detailed study of apatites from the Kaiserstuhl alkaline complex, Germany, and suggested that up to 60% of the PO₄³⁻ ions may be replaced by SiO₄⁴⁻ and CO₃²⁻-CO₃OH³⁻. They argued that a complete solid solution series of silicate-carbonate-hydroxylapatite may exist in nature and may be described by the following simplified formula: (Ca,Sr,LREE)₁₀[(SiO₄)_x(CO₃)_x(PO₄)_{6-2x}]

(OH,F)₂, where LREE represents the light rare earth elements (Ce, La, and Nd).

In contrast, Wallaey (1954), Bonel and Montel (1964), and Elliott (1965) suggested that in certain apatite the CO₃²⁻ ions replace the OH⁻ ions within the apatite structure. On the basis of experimental results, they argued that apatite exposed to a CO₂ atmosphere at temperatures of 1000 °C shows a positive correlation between the carbonate content and the *a*-axis parameter, suggesting that the CO₃²⁻ ions replace the OH⁻ ions within the apatite structure. The experiments presented here suggest that the carbonate replaces the PO₄³⁻ ion in the apatite structure, but they do not indicate whether we have a simple substitution of PO₄³⁻ for CO₃²⁻ and how other elements are arranged in the structure in order to maintain the charge balance. Although there is evidence that carbonate occupies the phosphate site in the apatite structure, there may not be a unique way by which CO₂ is incorporated into the apatite structure, but there may be a series of mechanisms that may depend on fluid composition in addition to temperature and pressure conditions.

Apatite is one of the few minerals that have been used to determine fluid composition in high-temperature rocks, mainly with regard to the concentration of Cl and F in solution (Stormer and Carmichael, 1971; Yardley, 1985; Andersen and Austrheim, 1991; Brenan, 1993). The results presented above show that apatite may also be a potential tool to determine the CO₂-H₂O ratio of geological fluids, although it is not yet clear what are the main mechanisms and conditions that control the formation of carbonate-bearing apatites under high temperature and pressure. The laboratory experiments described here suggest that there is not a simple relationship between the concentration of CO₂ in the apatite structure and in the coexisting fluid phase. However, there seems to be a difference in the concentration of CO₂ in apatite formed in the presence of H₂O-CO₂-bearing fluids and in apatite formed with carbonate-bearing fluids (Table 5). Although more experiments are necessary to clarify this observation, it appears that apatites formed in the presence of carbonate, either CaCO₃ or Na₂CO₃, have, in general, CO₂ contents of approximately 0.35 wt%, whereas apatites formed in the presence of H₂O-CO₂ fluids have CO₂ contents below that value.

A major question in the study of carbonatites is the extent to which the fluids emanating from the carbonate magma affect the host rock. The results of this study show that in Jacupiranga the carbonate-rich apatite (up to 0.8 wt% CO₂) is restricted to rocks affected by metasomatic fluids. Examples of these rocks are the pegmatoid rocks related to the emplacement of the carbonatite and the narrow zone of feldspathic fenitization in the melteigites. If the CO₂ content of apatite in these rocks relates to carbonate-bearing fenitization fluids, one may suggest that carbonate metasomatism in Jacupiranga is restricted to the contact of the carbonatite with the magnetite clinopyroxenite and to narrow zones of feldspathization within the host rock.

ACKNOWLEDGMENTS

We thank Toshiko K. Mayeda for her technical assistance and support in the laboratory and R.C. Newton, who kindly provided assistance and laboratory equipment for the high-temperature and -pressure experiments. We also thank the Universidade Federal de Ouro Preto and Conselho Nacional de Desenvolvimento Científico e Tecnológico (CNPq grant 20.0594/89.3) for providing scholarship and financial support to R.V.S. This study was also supported by National Science Foundation grant EAR-9218857 to R.N.C. and EAR-9015581 to R.C. Newton.

REFERENCES CITED

- Ames, L.L., Jr. (1959) The genesis of carbonate apatites. *Economic Geology*, 54, 829–841.
- Andersen, T., and Austrheim, H. (1991) Temperature-HF fugacity trends during crystallization of calcite carbonatite magma in the Fen Complex, Norway. *Mineralogical Magazine*, 55, 81–94.
- Ando, J., and Matsuno, S. (1968) Ca₃(PO₄)₂-CaNaPO₄ system. *Bulletin of the Chemical Society of Japan*, 41, 342–347.
- Arends, J., and Davidson, C.L. (1975) HPO₄²⁻ content in enamel and artificial carious lesions. *Calcified Tissue Research*, 18, 65–79.
- Baddiel, C.B., and Berry, E.E. (1966) Spectra-structure correlation in hydroxyapatites and fluorapatites. *Spectrochimica Acta*, 22, 1407–1416.
- Bhatnagar, V.M. (1967) IR spectra of fluorapatite and the fluorochlorapatite. *Experientia*, 23, 10–12.
- (1968) IR spectra of hydroxyapatite and fluoroapatite. *Bulletin de la Société Chimique de France Special Issue*, 1771–1773.
- Binder, G., and Troll, G. (1989) Coupled anion substitution in natural carbon-bearing apatites. *Contributions to Mineralogy and Petrology*, 101, 394–401.
- Bonel, G., and Montel, G. (1964) Sur une nouvelle apatite carbonatée synthétique. *Comptes Rendus de l'Académie des Sciences de Paris*, 258, 923–926.
- Brenan, J.M. (1993) Partitioning of fluorine and chlorine between apatite and aqueous fluids at high pressure and temperature: Implications for the F and Cl content of high *P-T* fluids. *Earth and Planetary Science Letters*, 117, 251–263.
- Chickerur, N.S., Tung, M.S., and Brown, W.E. (1980) A mechanism for incorporation of carbonate into apatite. *Calcified Tissue International*, 32, 55–62.
- Elliott, J.C. (1965) The interpretation of the infra-red absorption spectra of some carbonate-containing apatites. In M.V. Stack and R.W. Fearnhead, Eds., *Tooth enamel: Its composition, properties, and fundamental structure*, p. 20–58. Wright, Bristol, U.K.
- Featherstone, J.D.B., Pearson, S., and LeGeros, R.Z. (1984) An infrared method for quantification of carbonate in carbonated apatites. *Caries Research*, 18, 63–66.
- Freund, F., and Knobel, R.M. (1977) Distribution of fluorine in hydroxyapatite studied by infrared spectroscopy. *Journal of the Chemical Society, Dalton Transactions*, 12, 1136–1138.
- Fridmann, S.A. (1967) Pelleting techniques in infrared analysis: A review and evaluation. In H.A. Szymanski, Ed., *Progress in infrared spectroscopy*, vol. 3, p. 1–23. Plenum, New York.
- Groves, A.W. (1951) *Silicate analysis: A manual for geologists and chemists, with chapters on check calculations and geochemical data* (2nd edition), 336 p. Allen and Unwin, London.
- Gulbrandsen, R.A., Kramer, J.R., Beatty, L.B., Mays, R.E. (1966) Carbonate-bearing apatite from Faraday Township, Ontario, Canada. *American Mineralogist*, 51, 819–824.
- Holager, J. (1972) Thermogravimetric experiments on tooth carbonates. *Journal of Dental Research*, 51, 102–106.
- LeBas, M.J., and Handley, C.D. (1979) Variation of apatite composition in ijolitic and carbonatitic igneous rocks. *Nature*, 279(3), 54–56.
- LeGeros, R.Z. (1965) Effects of carbonate on the lattice parameter of apatite. *Nature*, 206, 403–404.
- LeGeros, R.Z., Trautz, O.R., LeGeros, J.P., and Klein, E. (1968) Carbonate substitution in the apatite structure I. *Bulletin de la Société Chimique de France Special Issue*, 1712–1718.
- McClellan, G.H., and Lehr, J.R. (1969) Crystal chemical investigation of natural apatites. *American Mineralogist*, 54, 1374–1391.

- McCrea, J.M. (1950) On the isotopic chemistry of carbonates and a paleotemperature scale. *Journal of Chemical Physics*, 18, 849–857.
- Nelson, D.G.A., and Featherstone, J.D.B. (1982) Preparation, analysis, and characterization of carbonated apatites. *Calcified Tissue International*, 34, S69–S81.
- Okazaki, M. (1983) F⁻-CO₃²⁻ interaction in IR spectra of fluoridated CO₃-apatites. *Calcified Tissue International*, 35, 78–81.
- Prins, P. (1973) Apatite from African carbonatites. *Lithos*, 6, 133–144.
- Silverman, S.R., Fuyat, R.K., and Weiser, J.D. (1952) Quantitative determination of calcite associated with carbonate-bearing apatites. *American Mineralogist*, 37, 211–222.
- Sommerauer, J., and Katz-Lehnert, K. (1985) A new partial substitution mechanism of CO₃²⁻/CO₃OH³⁻ and SiO₄⁴⁻ for PO₄³⁻ group in hydroxy-apatite from the Kaiserstuhl alkaline complex (SW-Germany). *Contributions to Mineralogy and Petrology*, 91, 360–368.
- Stormer, J.C., Jr., and Carmichael, I.S.E. (1971) Fluorine-hydroxyl exchange in apatite and biotite: A potential igneous geothermometer. *Contributions to Mineralogy and Petrology*, 31, 121–131.
- Stormer, J.C., Jr., Pierson, M.L., and Tacker, R.C. (1993) Variation of F and Cl X-ray intensity due to anisotropic diffusion in apatite during electron microprobe analysis. *American Mineralogist*, 78, 641–648.
- Wallaey, R. (1954) Etude d'une apatite carbonatée obtenue par synthèse dans l'état solide. In *Silicium, sulphur, phosphates. Colloquium of the International Union of Pure and Applied Chemistry, Münster*, p. 183–190. Verlag Chemie, Weinheim, Germany.
- White, W.B. (1974) The carbonate minerals. In V.C. Farmer, Ed., *The infrared spectra of minerals*, chapter 12, p. 227–284. Mineralogical Society, London.
- Yardley, B.W.D. (1985) Apatite composition and the fugacities of HF and HCl in metamorphic fluids. *Mineralogical Magazine*, 49, 77–79.

MANUSCRIPT RECEIVED MARCH 30, 1994

MANUSCRIPT ACCEPTED DECEMBER 5, 1994